1 **Particulate trace metal dynamics in response to increased CO_2 and iron availability in a**

2 **coastal mesocosm experiment**

4 M. Rosario Lorenzo[1], María Segovia[1], Jay T. Cullen[2], and María T. Maldonado[3]

6 [1]Department of Ecology, Faculty of Sciences, University of Málaga, Bulevar Louis Pasteur s/n, 29071-Málaga, Spain

7 [2]School of Earth and Ocean Sciences, University of Victoria, 3800 Finnerty Road, A405, Victoria BC V8P 5C2

8 Canada

9 [3]Department of Earth, Ocean and Atmospheric Sciences, University of British Columbia, 2207 Main Mall, Vancouver

10 BC V6T 1Z4, Canada

12 *Correspondence to:* María Segovia (segovia@uma.es) and María T. Maldonado (mmaldonado@eoas.ubc.ca)

14 **Abstract.** Rising concentrations of atmospheric carbon dioxide are causing ocean acidification and will influence

15 marine processes and trace metal biogeochemistry. In June 2012, in Raunefjord (Bergen, Norway) we performed a

16 mesocosm experiment, comprised of a fully factorial design of ambient and elevated pCO_2 and/or an addition of the

17 siderophore desferrioxamine B (DFB). In addition, the macronutrient concentrations were manipulated to enhance a

18 bloom of the coccolithophore *Emiliania huxleyi*. We report here the changes in particulate trace metal concentrations

19 during this experiment. Our results show that particulate Ti and Fe were dominated by lithogenic material while

20 particulate Cu, Co, Mn, Zn, Mo and Cd had a strong biogenic component. Furthermore, significant correlations were

21 found between particulate concentrations (mol L^{-1}) of Cu, Co, Zn, Cd, Mn, Mo, and P in seawater and phytoplankton

22 biomass (μgC L^{-1}), supporting a significant influence of the bloom in the distribution of these particulate elements. The

23 concentrations of these biogenic metals (mol L^{-1}) in the *E. huxleyi* bloom were ranked as: Zn > Cu $\approx$ Mn > Mo > Co >

24 Cd. Changes in CO_2 affected total particulate concentrations (mol L^{-1}) and biogenic metal ratios (Me:P) for some

25 metals, while the addition of DFB only affected significantly the concentrations of some particulate metals (mol L^{-1}

26).Variations in CO_2 had the most clear, and significant effect on particulate Fe concentrations (mol L^{-1}), decreasing its

27 concentration under high CO_2. Indeed, high CO_2 and/or DFB promoted the dissolution of particulate Fe, and the

28 presence of this siderophore helped maintaining high dissolved Fe. This shift between particulate and dissolved Fe

29 concentrations, in the presence of DFB, promoted a massive bloom of *E. huxleyi* in the treatments with ambient CO_2.

30 Furthermore, high CO_2 decreased the Me:P ratios of Co, Zn and Mn, while increased the Cu:P ratios. These findings

31 support theoretical predictions that the Me:P ratios of metals whose seawater dissolved speciation is dominated by free

32 ions (e.g. Co, Zn and Mn) will likely decrease or stay constant under ocean acidification. In contrast, high CO_2 is

33 predicated to shift the speciation of dissolved metals associated with carbonates, such as Cu, increasing their

34 bioavailability, and resulting in higher Me:P ratios.

35

36

37 *Key words:* Global change, Fe, CO_2, particulate trace metals, dissolved trace metals, mesocosms, *Emiliania huxleyi,*

38 phytoplankton

39

1. Introduction

Marine phytoplankton contribute half of the world's total primary productivity, sustaining marine food webs and driving the biogeochemical cycles of carbon and nutrients (Field et al., 1998). Annually, phytoplankton incorporate approximately 45 to 50 billion metric tons of inorganic carbon (Field et al., 1998), removing a quarter of the CO_2 emitted to the atmosphere by anthropogenic activities (Canadell et al., 2007). Yet, the atmospheric CO_2 concentration has increased by 40 % since pre-industrial times as a result of anthropogenic CO_2 emissions, producing rapid changes in the global climate system (Stocker et al., 2013). The dissolution of anthropogenic CO_2 in seawater, causes shifts in the carbonate chemical speciation, and leads to ocean acidification (OA). Marine ecosystems are sensitive to changes in pH because pH strongly affects chemical and physiological reactions (Hoffman et al., 2012). Increased CO_2 in seawater may enhance or diminish phytoplankton productivity (Mackey et al., 2015), decrease the $CaCO_3$ production in most planktonic calcifiers (Riebesell and Tortell 2011), and/or inhibit organic nitrogen and phosphorus acquisition (Hutchins et al., 2009). Thus, the biogeochemical cycling of nutrients is predicted to be highly affected by OA (Hutchins et al. 2009), as well as the distribution and speciation of trace metals in the ocean (Millero et al., 2009).

Trace metals, including Fe, Zn, Mn, Cu, Co and Mo, are essential for biological functions (e.g. photosynthesis, respiration and macronutrient assimilation), and Cd can supplement these functions. Trace metals availability can influence phytoplankton growth and community structure (Morel and Price, 2003). In turn, plankton control the distribution, chemical speciation, and cycling of trace metals in the sea (Sunda, 2012), by, for example, releasing organic compounds that dominate the coordination chemistry of metals, internalizing trace elements into the cells, and reducing and/or oxidizing metals at the cell surface. The chemistry of redox speciation of active trace metals is highly dependent on pH.   Fe occurs in two main redox states in the environment: oxidized ferric Fe (Fe (III)), which is poorly soluble at circumneutral pH; and reduced ferrous Fe (Fe (II)), which is   more soluble in natural seawater, but becomes rapidly oxidized (Millero et al. 1987). Fe speciation and bio- availability are dynamically controlled by the prevalent changing redox conditions. Also, as the ocean becomes more acidic, reduction of Cu (II) will increase, as the ionic form of Cu (II) is reduced to Cu (I) (Millero et al., 2009). The effect of higher concentrations of Cu (I) in surface waters on biological systems is not well known. Therefore, while the effects of OA on inorganic metal speciation will be more pronounced for metals that form strong complexes with carbonates (e.g. copper) or hydroxides (e.g. Fe and aluminium), those that form stable complexes with chlorides (e.g. cadmium) will not be greatly affected. pH mediated changes in concentrations and/or speciation could possibly enhance trace metals limitation and/or toxicity to marine plankton (Millero et al., 2009).

Fe is crucial for phytoplankton growth because   it is involved   in many essential physiological processes, such as photosynthesis, respiration, and nitrate assimilation (Behrenfeld and Milligan, 2013). The decrease in seawater pH in response to OA may increase Fe solubility (Millero et al., 2009), but it may also result in unchanged or lower Fe bioavailability, depending on   the nature of the strong organic Fe ligands (Shi et al., 2010). Consequently, changes in Fe bioavailability due to ocean acidification can affect positively or negatively ocean productivity and CO_2 drawdown. Copper is an essential micronutrient but may be toxic at high concentrations (Semeniuk et al., 2016). An increase in free cupric ion concentrations in coastal areas due to ocean acidification (Millero et al., 2009) could result in negative effects on phytoplankton. Given that trace metals are essential for phytoplankton productivity, and that they are actively internalized during growth, it is important to study the impacts of ocean acidification on the trace metal content of ecologically significant plankton species.

In a rapidly changing global environment, generated by anthropogenic CO_2 emissions, it is critical to gain adequate

83 understanding about ecosystem responses. Due to the complex interactions in aquatic ecosystems, such predictions have
84 so far not been possible to do based upon observational data and modelling alone. However, direct empirical studies on
85 natural communities offer a robust tool to analyse interactive effects of multiple stressors. Specifically, mesocosm
86 experiments allow perturbation studies with a high degree of realism compared to other experimental systems such as in
87 the laboratory (high controlled conditions usually far from reality) or *in situ* in the ocean (where not all the interactions
88 are contemplated) (Riebesell et al., 2010, Stewart et al., 2013, Riebesell and Gatusso, 2015).

90 In the present work a bloom of the coccolithophorid *Emiliania huxleyi* was induced in a mesocosm experiment in a
91 Norwegian fjord, where the speciation of particulate and dissolved trace metals is very dynamic (e.g. Fe; Ozturk et al.
92 2002). We aimed to examine and characterize the change of particle trace metals during an E. huxleyi bloom under the
93 interactive effects of increased CO_2 and/or dissolved Fe. *Emiliania huxleyi* is the most cosmopolitan and abundant
94 coccolithophore in the modern ocean (Paasche, 2002) and its growth and physiology has been studied under this
95 experimental conditions (Segovia et al., 2017, Segovia et al., 2018, Lorenzo et al., 2018). Furthermore, *E. huxleyi* has
96 unique trace metal requirements relative to other abundant phytoplankton taxa (ie. diatoms or dinoflagellates; Ho et al.
97 2003). Coccolithophores play a key role in the global carbon cycle because they produce photosynthetically organic
98 carbon, as well as particulate inorganic carbon through calcification. These two processes foster the sinking of
99 particulate organic carbon—and trace metals—and contribute to deep ocean carbon export (Hutchings, 2011) and
100 ultimately to organic carbon burial in marine sediments (Archer, 1991, Archer and Maier-Reimer., 1994). However,
101 ocean acidification will disproportionally affect the abundance of coccolithophores, as well as their rates of
102 calcification and organic carbon fixation (Zondervan et al., 2007). The aim of the present study was to characterize the
103 changes in particulate trace metal concentrations—in both lithogenic and biogenic particles— during a bloom of
104 *E. huxleyi* under realistic changes in CO_2 and Fe bioavailability expected by 2100.

2. Materials and methods

2.1 Experimental set-up

109 The experimental work was carried out in June 2012 in the Raunefjord, off Bergen, Norway as described in detail by
110 Segovia et al., (2017). Twelve mesocosms (11 m^3 each) were set-up in a fully factorial design with all combinations of
111 ambient and elevated pCO_2 and dFe in three independent replicate mesocosms. The mesocosms were covered by lids
112 (both transparent to PAR and UVR) and filled with fjord water from 8 m depth. We achieved two CO_2 levels
113 corresponding to present (390 ppm, LC) and those predicted for 2100 (900 ppm, HC) by adding different quantities of
114 pure CO_2 gas (Shculz et al., 2009). The specific CO_2 concentration and the CO_2 inlet flows in the mesocosms were
115 measured by non-dispersive infrared analysis by using a Li-Cor (LI-820) CO_2 gas analyser (Li-COR, Nebraska, USA).
116 CO_2 concentrations in the mesocosms were calculated from pH and total alkalinity measurements using the CO_2 SYS
117 software (Robbins et al,. 2010). At the beginning of the experiment, nitrate (10 μM final concentration) and phosphate
118 (0.3 μM final concentration) were added to induce a bloom of the coccolithophore *Emiliania huxleyi*, according to Egge
119 & Heimdal (1994). Following recommendations by Marchetti and Maldonado (2016), t o induce changes in Fe
120 availability, and analyse its effects on the plankton community, 70 nM (final concentration) of the siderophore
121 desferrioxamine B (DFB) (+DFB and −DFB treatments) (Figure S1b-supplemental material) was added to half of the
122 mesocosms on Day 7, when the community was already acclimated to high CO_2. The initial dFe concentration before
123 DFB addition was about 4.5 nM. Even though DFB is a strong Fe-binding organic ligand often used to induce Fe
124 limitation in phytoplankton (Wells 1999), DFB additions may also in- crease the dissolved Fe pool in environments
125 with high concentrations of colloidal and/or particulate Fe, such as fjords (Kuma et al. 1996, Öztürk et al. 2002). By day

17, dissolved Fe concentrations were significantly higher (by ~3-fold) in the high CO_2 and DFB treatments than in the control (Segovia et al. 2017). These results support an increase in the solubility of Fe in seawater by either lowering its pH (Millero 1998; Millero et al. 2009) and/or the addition of DFB (Chen et al. 2004). The multifactorial experimental design consisted of triplicate mesocosms per treatment and the combinations of high and ambient pCO_2 and dFe levels, resulted in a total of 12 mesocosms: LC-DFB (control), LC+DFB, HC+DFB and HC-DFB. Water samples from each mesocosm were taken from 2 m depth by gentle vacuum pumping of 25 L volume into acid-washed carboys that were quickly transported to the onshore laboratory. The biological and chemical variables analysed were phytoplankton abundance and species composition, dissolved Fe and Cu concentrations (dFe, dCu), nutrient concentrations (nitrate, phosphate, silicic acid and ammonium) and particulate trace metal concentrations.

2.2 Dissolved copper (dCu)

Low density polyethylene (LDPE) bottles were cleaned with 1% alkaline soap solution for one week, then filled with 6 M trace metal grade HCl (Seastar, Fisher Chemicals) and submerged in a 2 M HCl bath for one month. For transport, they were filled with 1 M trace metal grade HCl for one more month and kept double bagged. In between each acid treatment, the bottles were rinsed with Milli-Q water (Millipore; hereafter referred to as MQ). Before sampling, the bottles were rinsed three times with filtered seawater. Seawater was collected from each mesocosm, filtered through 0.2 μm AcroPak Supor membrane capsule filters into the trace metal clean LDPE bottles, and acidified with ultra-clean trace metal grade HCl in a Class 100 laminar flow hood. Total dissolved Cu concentrations were measured following Zamzow et al., (1998) using a flow injection analysis chemiluminescence detection system (CL-FIA, Waterville Analytical). Total dissolved Fe concentrations were measured as described in Segovia et al., (2017) for this very experiment.

2.3 Particulate metals (pMe)
2.3.1 Sampling
All equipment and sampling material used during this study was rigorously acid-washed under trace metal clean conditions and protocols according to GEOTRACES . The material was cleaned with Milli-Q water (MQw) with 10 % Extran (Fisher Chemicals) at 60°C for 6h, followed by 3 thorough rinses with MQw at room T. The material was then cleaned with 10 % HPLC grade HCl (Sigma-Aldrich) at 60°C or 12h and then rinsed thoroughly 5 times with MQw at room T. The material was then covered by plastic and transported to the raft. Sampling in the raft was carried out under a mobile plastic cover hood. Filters were precleaned with 10% trace metal grade hydrochloric acid (Seastar, Fisher Chemicals), at 60°C overnight and were rinsed with MQw. Seawater samples (1-3.5 L) were filtered gently onto 0.45 μm acid washed Supor ®-450 filters (within a trace metal clean Swinnex filter holder) on days 12, 17 and 21 of the experiment. Four technical replicates were taken from each mesocosm. Two filters were analysed without manipulation and the other two were individually washed with oxalate-EDTA reagent to remove extracellular Fe, as well as other metals (Tang and Morel, 2006). Immediately following filtration, the treated filters were soaked with 20 mL EDTA–oxalate solution, added to the headspace of the Swinnex holders, with an acid-washed polypropylene syringe. After 10 min, vacuum was applied to remove the oxalate solution and 10 mL of 0.2 μm filtered chelexed synthetic oceanic water (SOW) solution was passed through the filter to rinse off any remaining oxalate solution. Replicate filters that were not treated with oxalate solution were transferred directly to centrifuge tubes for storage. The filters with particles were frozen in acid-washed 2 mL polypropylene tubes and then, dried and stored until analysis.

2.3.2 Analytical methods

168 Filters were digested in 7-mL acid-washed Teflon (Teflon, Rochester, NY, USA) vials. Teflon vials were also

169 precleaned using 10% trace metal hydrochloric acid (Fisher, trace metal grade) during two days and then, with nitric

170 acid (Fisher, trace metal grade) at 70 ºC during three days. In between each acid treatment, the bottles were rinsed with

171 MQ. Samples were digested in 3 mL of HNO_3 and 0.5 mL of HF (Fisher, trace metal grade) with lids on for 1 h on a

172 hot plate at 200 ºC. The lids were then removed to evaporate HF at 200ºC. After this, 1.5 mL of HNO_3 were added and

173 the samples were heated with lids on overnight at 150 ºC. Finally, 2.25 mL of $HClO_4$ (Fisher, Optima grade) were

174 added and the samples were heated for 4 h at 200 ºC. After complete digestion, the samples were dried on hot plates at

175 200ºC. The dried samples were dissolved in 1% nitric acid with 1 ppb in internal standard. The analysis was performed

176 using a high-resolution inductively coupled plasma-mass spectrometer (ICP-MS, Element XR, Thermo Scientific) and

177 the described instrumental settings (Table S1). Filter blanks were collected and subjected to the same storage, digestion,

178 dilution, and analysis processes, and these blank values were subtracted from sample measurements. Particulate

179 samples for ICP-MS analysis were processed in a trace metal-clean laboratory under a trace metal-clean laminar flow

180 fume hood.

181

182 **2.3.3 The effect of oxalate-EDTA wash on particulate trace metal concentrations**

183 To better estimate the biogenic fraction of the particulate metals, the filters were washed with an oxalate-EDTA

184 solution, which removes extracellular metals and oxyhydroxides (Tovar-Sanchez et al., 2003; Tang and Morel, 2006).

185 In our study, the oxalate wash significantly decreased the concentration of all particulate metals, with the exception of

186 Al and Ti (Tables S2 and S3), as observed by Rauschenberg and Twining (2015). The quantity of metal remaining after

187 the oxalate wash (i.e. biogenic fraction) varied among elements (Tables S2 and S3). In general, the concentrations of Fe

188 and Co in the particles were decreased the least by the oxalate wash by ~ 25%, while Mo and Pb concentrations were

189 decreased the most by ~70%. The concentrations of particulate Cu, Zn, Cd and Mn were reduced by 50% by the oxalate

190 wash. As shown previously (Sanudo-Wilhelmy et al. 2004), the oxalate reagent also removed extracellular P (by ~20%,

191 Table S2 & S3). Compared to Rauschenberg and Twining (2015), the estimates of the biogenic fraction, after the

192 oxalate wash, were in agreement for Co, Cu and P, and lower for Fe, Mn, Zn and Cd concentrations.

193

194 However, the efficacy of the oxalate wash to dissolve Fe, and other metals, from lithogenic particles is not well

195 constrained (Frew et al. 2006, Rauschenberg and Twining., 2015, King et al., 2012). Therefore, the results obtained

196 after the oxalate-EDTA wash should be interpreted with caution because we do not know whether the removed metal

197 fraction is a) only lithogenic; b) mainly lithogenic but some biogenic fraction is also removed, or c) whether metals

198 absorbed onto particles are equally labile to the wash on biogenic and lithogenic particles. Given that many of the

199 trends we observed were identical for the oxalate-EDTA washed and non-washed particles [i.e. higher Me

200 concentrations in the LC+DFB treatments (Table S2 & S3) and positive correlations between phytoplankton biomass

201 and Me concentrations (Lorenzo-Garrido 2016)], below we present and discuss only the non-oxalate wash results.

202

203 **2.4 Statistical analyses**

204 Data were checked for normality (by Shapiro-Wilks' test), homoscedasticity (by Levene's test) and sphericity (by

205 Mauchly's test). All data met the requirements to perform parametric tests. Statistical significance of treatment effects

206 was carried out using Split-Plot ANOVA followed by post-hoc Sidak and Bonferroni tests (considering $P < 0.05$ as

207 significant). All analyses were performed using the General Linear Model (GLM) procedure. The correlation between

208 variables was analysed by Pearson's product-moment multiple comparisons (considering $P < 0.05$ as significant).

209 Statistical analyses were carried out using SPSS v22 (IBM statistics) and Sigmaplot 12 (Systat Software, Chicago,

210 USA).

3. Results

3.1 Biological and chemical characteristics during the bloom

Plankton community dynamics and their response to the applied treatments in the mesocosms are described in detail by Segovia *et al.* (2017). Briefly, at the beginning of the experiment (days 1-10) a bloom of large chain-forming diatoms was observed, which declined by day 7 (Figure S1g- supplemental material). This diatom bloom was associated with a sharp decrease in nitrate and silicic acid concentrations (Figure S2-supplemental material). Picoeukaryotes, dominated the phytoplankton community on day 8 (Figure S1d). During the first 10 days of the experiment, there were no significant differences in the chemical variables measured between the treatments (Figures S3 and S2 -supplemental material). On day 7, half of the mesocosms were amended by adding DFB (+DFB treatments). Between day 7 and 17, an increase in dFe was observed in all treatments, except in the control (Figure S3). This increase in dFe was sustained for the entire experiment in the DFB treatments (Figure S3). Dissolved Cu concentrations were not affected by the different treatments (Figure S3). After day 10, a massive bloom of the coccolithophore *E. huxleyi* developed under LC +DFB condition (Figure S1b), out-competing the rest of the plankton groups (Figure S1). This bloom was not observed either in the control treatment (LC-DFB) or in the HC treatments, although *E. huxleyi* was still the most abundant species in all treatments; with the exception of the HC-DFB treatment (Figure S1b).

3.2 Particulate metal concentrations during the mesocosm experiment

The pMe concentrations (nM, mean of all treatments and dates) during the experiment were highest for Al, Fe and Zn, and lowest for Cd, following this trend: Al ≈ Fe ≈ Zn > Ti > Cu ≈ Mn > Mo ≈ Pb > Co > Cd (Figure 1, Table S2). Significant changes over time were observed for all particulate trace metal concentrations (Fe, Cu, Co, Zn, Cd, Mn, Mo and Pb), except for Ti and Al (Figure 1, Table 1). The only metal that showed a significant time-dependent decrease in its particulate concentration was Fe (Figure 1, Table 1). In general, the treatments with the highest particulate metals concentrations also exhibited the highest particulate P, except for Al, Ti, Fe, and Pb (Figure 1, Table S2). On days 12 and 17, the highest particulate metals concentrations were observed in the LC+DFB treatment, while on day 21, they were observed in both LC treatments (Figure 1, Table S2).

3.3 The effects of increased CO_2 and the DFB addition on particulate metal concentrations

Increased CO_2 and the DFB addition did not significantly affect the concentrations of particulate Al, Ti, Cu, and Pb (Tables 1and S2). Similarly, the addition of DFB did not directly influence particulate concentrations of Fe, but high CO_2 had a significant negative impact on particulate Fe (Tables 1 and S2, Figure 1). Particulate Cd concentrations were also inversely affected by CO_2, but only in the presence of DFB (CO_2; and CO_2 x DFB effect, Tables 1 and S2, Figure 1). All other elements (P, Co, Zn, Mn and Mo) exhibited significant effects by CO_2 and by DFB, but there was also a significant interaction between these two factors (Table 1, S2). This indicates that, for example, particulate Mn, Zn, Mo, Co, and P concentrations were significantly decreased by high CO_2, but only in the +DFB treatments (Figure 1, Table 1, S2,). Similarly, the addition of DFB significantly increased pZn and pMn, but only at ambient CO_2 levels (Figure 1, Tables 1, S2).

3.4 Phosphorous-normalized metal ratios in particles collected from the mesocosms and the effects of increased CO_2 and the DFB addition on these ratios

The P-normalized metal ratios (Figure 2 and means in Table 2) were highest for Al and Fe (mean: 70 ± 38 mmol Al: mol P, and 39 ± 34 mmol Fe: mol P), and lowest for Cd and Co (mean 0.02 ± 0.01 mmol Cd: mol P, and 0.07 ± 0.02 mmol Co: mol P). Fe:P and Ti:P were not significantly affected by increased CO_2 and/or the DFB addition, but showed a significant decrease over time (Table 3). The P-normalized Cu, Co and Zn ratios changed significantly over time

254 (Table 3). Increased CO_2 significantly decreased Co, Zn and Mn:P ratios, while it increased Cu:P ratios (Figure 2, Table

255 3). DFB did not affect the Me:P ratios of any of these bioactive elements (Table 3).

256

257 **4. Discussion**

258 **4.1 The effects of CO_2 and dFe on the plankton community**

259 In this experiment we investigated changes in particulate trace metal concentrations, in response to increased CO_2

260 and/or an addition of the siderophore DFB in a coastal mesocosm experiment. For a better understanding of the

261 processes affecting these stressors, we briefly summarise the mesocosm experiment results originating from Segovia et

262 al. (2017). High CO_2, as well as the DFB addition increased dFe concentration. The higher dFe concentrations were

263 sustained in the DFB treatments. A bloom of the coccolithophore *Emiliania huxleyi* was observed in the ambient CO_2

264 treatments, and was especially massive in the one with the addition of DFB (LC+DFB).   Indeed, the biomass of *E.*

265 *huxleyi* was negatively affected by increased CO_2. However, increased dFe partially mitigated the negative effect of

266 elevated CO_2, indicating that the coccolithophore was able to acclimate better to ocean acidification when Fe

267 availability was high. High dFe also had a positive effect on the cyanobacterium *Synechococcus sp*, while the rest of the

268 plankton food web did not response to the treatments (Segovia et al. 2017).

269 **4.2 Particulate Fe and Ti are associated with lithogenic sources, while particulate Co, Cu, Zn, Cd, Mo and Mn**

270 **are associated with biogenic sources**

271 The particulate trace metal concentrations (nM, mean of all treatments and dates) during the experiment were highest

272 for Al, Fe and Zn, and lowest for Co and Cd, following this trend: Al ≈ Fe ≈ Zn > Ti > Cu ≈ Mn > Mo ≈ Pb > Co > Cd.

273 Lithogenic particles are enriched in Al and low in P (average crustal Al and P content is 2.9 mmol Al and 0.034 mmol

274 P g^{-1} dry weight, Taylor 1964), while biogenic particles are enriched in P and low in Al (average plankton Al and P

275 content is 0.001 mmol Al and 0.26 mmol P g^{-1} dry weight, Bruland et al. 1991). Therefore, the distinct high abundance

276 of Al and P in lithogenic and biogenic particles, respectively, can be used to evaluate the relative contribution of

277 lithogenic and biogenic material in our particulate samples. In order to do this, first, it is important to establish that the

278 vast majority of the measured particulate P is associated the biogenic fraction. In this study, the abiotic P was estimated

279 using particulate Al concentrations (nM) and the P:Al ratio in crustal material, and was calculated to be negligible (<

280 1% of the total measured particulate P). In addition, a significant correlation (p< 0.003) was found between particulate

281 P concentrations and phytoplankton biomass (Table 4). Therefore, we assume a constant trace metal composition in

282 biogenic particles (assuming they are rich in phytoplankton) and lithogenic particles (assuming they are rich in crustal

283 material). We then calculated the expected metal concentrations in the particulate samples assuming that all the P

284 measured in the particles is associated with a biogenic fraction, and that all Al in the particles is associated with the

285 lithogenic fraction. Thus, for a given trace metal, its expected particulate trace metal concentration in seawater (mol L^{-1}

286 ^{1}) can be calculated as the sum of the contribution from biogenic and lithogenic particles, so that:

287

288 $[Me] = a\,[P] + b\,[Al]$

289

290 where [Me] is the total concentration of the metal (mol L^{-1}) expected in the particulate sample; [P] is the P

291 concentration measured in the particles (mol L^{-1}); [Al] is the Al concentration measured in the particles (nM L^{-1}); a is

292 the average, well-known metal content in biogenic particles, normalized to P (i.e. mol Me: mol P in marine plankton;

293 Ho 2006) and b is the average, well known metal content in lithogenic particles, normalized to Al (mol Me: mol Al in

294 the Earth crust; Taylor 1964). For example, on day 21 in the HC-DFB treatment, the concentrations of particulate Al

295 and P were 8.22 and 134.8 nM, respectively (Table S2). Assuming a constant 0.0051 mol Fe: mol P in biogenic

296   particles (Ho 2006) and 0.331 mol Fe: mol Al in lithogenic particles (Taylor 1964; Table 2), we calculated an expected

297   particulate Fe concentration of 3.41 nM, where 80% was associated with lithogenic material and 20% with biogenic

298   material. Similar calculations were made for the bioactive metals Mn, Co, Cu, Zn, Cd, and Mo (Table 2). Our

299   calculations indicate that on average, particulate Fe was dominated by the lithogenic component (accounting for an

300   average of 78% of the total expected particulate Fe), while for particulate Co, Cu, Zn, Cd, and Mo the biogenic fraction

301   dominated (accounting for 94, 95, 99, 94 and 98%, respectively, of the total expected concentration; Table 2).

302   Particulate concentrations of Mn were also dominated by the biogenic fraction (65% of the total), but the lithogenic

303   fraction was also significant (35%). Moreover, the expected particulate Mn and Fe concentrations closely matched the

304   particulate Mn and Fe concentration we measured (accounting for an average of ~ 71% of the measured Mn, and 115%

305   of the measured Fe). For other metals (i.e. Cu, Mo and Zn), the expected particulate concentrations (nM) were lower

306   than measured (23% of the measured pCu, and 8% of measured pZn; Table 2). This suggests that the particles were

307   enriched in Cu, Mo, and Zn relative to what is expected based on natural marine plankton metal quotas (Bruland et al.

308   1991) and crustal ratios (Taylor 1964).

309

310   To further establish the lithogenic or biogenic source of the pMe in the particles, the particulate metal concentrations

311   were normalized to the concentrations of particulate P and Al (Figure 2, and Table 2). These ratios were then compared

312   with well-known molar ratios of metal to Al in the crust (Taylor 1964) and of metal to P ratios in marine plankton

313   samples (Ho 2006) and cultures (Ho et al. 2003) (Table 2). The average Fe: Al (506 mmol Fe: mol Al) and Ti:Al ratios

314   (119 mmol Ti: mol Al, Table 2) were relatively similar to crustal molar ratios (331 mmol Fe: mol Al and 39 mmol Ti:

315   mol Al; Taylor 1964). Additional evidence for the significant lithogenic component in particulate Ti and Fe was

316   gathered from Figure 3, where we plotted the molar ratios of the metals relative to P in the collected particles against

317   the Al:P ratios measured in those same particles. The slope of these data [(Fe:P)/(Al:P) = mol Me: mol Al] is the ratio

318   of Me:Al in the particles and can be compared to well-known Me:Al crustal ratio. Visually, if the data nicely fit the

319   Me:Al line for crustal material, these metals are mainly associated with the lithogenic component, as evident for Fe and

320   Ti (Figure 3). These combined results suggest that in our experiment, particulate Fe and Ti concentrations were

321   enriched by lithogenic material. In support of this finding, we also found no significant correlation between particulate

322   Fe and Ti concentrations (nM) and either the total plankton (phytoplankton and microzooplankton) or *E. huxleyi*

323   biomass (μg C L^{-1}; Table 4).

324

325   In contrast, when the P-normalized metal ratios in the particles collected from the mesoscosms were plotted against the

326   Al:P ratios in these particles, there were no correlations for the following metals Co, Cu, Zn, Cd, Mn and Mo (Figure

327   4), indicating that these particulate metals were not enriched in lithogenic material. Our measured metal: P ratios were

328   comparable to plankton ratios in natural samples and in cultures (Table 2). The concentrations (mol L^{-1}) of these metals

329   (i.e. Cu, Co, Zn, Cd, Mn, Mo), as well as P, also showed significant correlations with the biomass (μgC L^{-1}) of *E.*

330   *huxleyi* and that of total plankton cells ($p < 0.05$, Table 4), supporting a significant influence of the phytoplankton in the

331   distribution of these particulate elements.

332

333   **4.3 Particulate metals with a strong biogenic component: their P-normalized ratios**

334   The concentrations of particulate bioactive metals (mol L^{-1}), with a significant biogenic component (i.e. excluding Fe)

335   in the studied *E. huxleyi* bloom were ranked as: Zn > Cu ≈ Mn > Mo > Co > Cd (Figure 1, Table S3), similar to those

336   reported in indigenous phytoplankton populations: Fe ≈ Zn > Cu ≈ Mn ≫ Co ≈ Cd, (Twining and Baines, 2013). The

337   only treatment where E. *huxleyi* did not dominate the community was the HC-DFB; in this treatment the ranking of

338   these biogenic particulate trace metals was the same as that of LC+DFB (with the massive *E. huxleyi* bloom), but their

339 concentrations were lower than those in LC+DFB. At the end of the experiment, the concentrations of these biogenic

340 metals were, in general, comparable in both HC treatments, and lower than those in the LC treatments (Figure 1, Table

341 S3). Therefore, high CO_2 had a tendency to decrease particulate metal concentrations, especially on day 21. Given the

342 strong correlation between concentrations of these particulate bioactive metals and phytoplankton biomass, the lower

343 particulate concentrations in high CO_2 were mainly due to low phytoplankton biomass.

344

345 Particulate Zn concentrations were especially high in the LC+DFB treatment (Figure 1), where the highest *E. huxleyi*

346 biomass was observed. *Emiliania huxleyi* is well known for its high Zn cellular requirements (~ 1-10 for *E. huxleyi* vs.

347 1-4 mmol Zn: mol P for other phytoplankton; Sunda and Hunstman 1995, Sunda 2013). But, the Zn: P ratios in the

348 LC+DFB treatment (range 45-69 mmol Zn: mol P; Figure 2, Table S2), as well as in all the other treatment (range 16-

349 34 mmol Zn: mol P; Figure 2, Table S2) were significantly higher than these published ratios. This could be explained

350 by, the adsorption of these metals to the outside of the cells, and/or anthropogenic inputs of Zn into the fjord. The Zn:P

351 ratios in the samples washed with the oxalate-EDTA were still high (range 28-57 for LC+DFB and 16-33 mmol Zn:

352 mol P in all other treatments, Table S3), thus adsorption might have not been significant. We hypothesize that

353 anthropogenic aerosols which are rich in anthropogenic particulate metals, such as Zn and Cu (Perry et al. 1999; Narita

354 et al. 1999), and have high percentage of Zn and Cu dissolution (ref.), might be the source of these high Zn

355 concentrations and ratios in the particles.

356

357 Similarly, the Cu:P ratios in the collected particles were relatively elevated (1.4 ± 0.8 mmol Cu: mol P) compared to

358 those of other phytoplankton, including *E. huxleyi* (Table 2). The dissolved (7.7±0.41 nM Cu, Figure S3) and

359 particulate Cu concentrations (0.35±0.25 nM, Table S2) in our experiment were high, and similar to those previously

360 measured in this fjord (Muller et al., 2005). Rain events (or wet deposition of anthropogenic aerosols) in this fjord result

361 in high dissolved Cu and the active production of strong organic ligands by *Synechococcus*—to lower the free Cu

362 concentrations (Muller et al., 2005). Therefore, high Cu might be a general condition in this fjord due to the rainy nature

363 of the geographical location, and indigenous plankton might have developed physiological mechanisms to deal with

364 high Cu, such as the production of organic ligands to prevent uptake (Vraspir and Butler, 2009), or of heavy-metal-

365 binding peptides (phytochelatins) to lower Cu toxicity inside the cell (Ahner and Morel, 1995; Ahner et al., 1995;

366 Knauer et al., 1998). Since we measured high particulate Cu, and Cu:P in our experiment, *E. huxleyi* might have been

367 relying mainly on phytochelatins to buffer high intracellular Cu (Ahner et al., 2002).

368

369 The Cd:P ratios (average 0.024 ± 0.01 mmol Cd:mol P, Figure 2) were significantly lower than those in phytoplankton

370 and *E. huxleyi* (0.36 mmol Cd:mol P, Figure 2). This was surprising, because Cd quotas are normally higher in

371 coccolithophores than in diatoms and chlorophytes (Sunda and Huntsman, 2000; Ho et al., 2003). High Cd quotas in

372 coccolithophores have been suggested to result from accidental uptake through Ca transporters and channels (Ho et al.,

373 2009). The low Cd quotas here may be explained by the antagonistic interaction between Mn and Cd or Zn and Cd

374 under high Mn and Zn, respectively (Sunda and Huntsman, 1998, 2000; Cullen and Sherrell, 2005).

375 Since high Zn:P ratios were common in this study (34.02 ± 18.05 mmol Zn:mol P, Figure 2), we hypothesize that high

376 Zn levels antagonistically interacted with Cd, resulting in low Cd:P ratios in the particles.

377

378 **4.4 The effects of increased CO_2 and the DFB addition on particulate metal concentrations and P-normalized**

379 **ratios**

380 Fe enrichment is common in coastal waters, due to sediment resuspension, rivers input, aeolian deposition and mixing

381 or upwelling of deep water. Indeed, Fe was the essential metal with the highest particulate concentrations in our study

382 (Figure 1, Table 3). Furthermore, in this study particulate Fe was characterized by a strong lithogenic component, and

383 was not correlated with phytoplankton biomass. Fe was also unique, in that it was the only trace element whose

384 particulate concentration was significantly and exclusively affected by CO_2 (no interaction between CO_2 and

385 DFB), regardless of the presence or absence of DFB (Table 1). Furthermore, particulate Fe concentrations (nM)

386 decreased steadily between days 12 and 21, with the exception of the control treatment (LC-DFB; Figure 1, Table 2S).

387 This suggests that the increase in CO_2 and/or the DFB addition reduce the concentration of pFe, despite the

388 phytoplankton bloom. Such a decrease in pFe (range 2.3-fold in LC-DFB, vs. 13.7-fold in HC+DFB; Table S2) might

389 be mediated by the dissolution of particulate Fe by low pH or by the presence of strong organic chelators as observed in

390 this very experiment (Segovia et al. 2017 and references therein) where dFe notably increased in treatments with high

391 CO_2 and/or the addition of DFB (Figure S3). Furthermore, the dissolution of particulate Fe in the treatments with high

392 CO_2 and/or the addition of DFB was evident in the Fe partitioning coefficients—the molar ratio between particulate and

393 dissolved concentrations (Figure 4). On day 21, the Fe partitioning coefficients varied by 22-fold between the highest

394 for the control (LC-DFB: 1.039) and lowest for the HC+DFB treatments (HC+DFB: 0.047; Figure 4). Thus, either the

395 DFB addition or high CO_2 promoted the dissolution of pFe. However, at the end of the experiment, high dFe

396 concentrations were only observed in the treatments with the DFB additions, suggesting that the presence of strong

397 organic Fe chelators, such as DFB, mediated the maintenance of high dissolved Fe concentrations, as previously

398 observed (Segovia et al. 2017). Thus, in our future oceans, high CO_2 (low pH) will increase dissolved Fe concentrations

399 in regions rich in particulate Fe, and in strong organic Fe chelators. The deleterious effects of OA on the development

400 of ecologically important species sensitive to increased CO_2 such as *E. Huxleyi*, will be more relevant in high-Fe

401 environments than in Fe-limited ones.

402 In contrast to the findings for Fe, particulate Cu concentrations a) were not affected by either high CO_2 or the DFB

403 addition; b) were dominated by a biogenic component and c) were significantly correlated with phytoplankton biomass

404 (Table 4). Furthermore, unique to Cu was a significant increase in Cu:P ratios by day 21 in the high CO_2 treatments,

405 especially when no DFB was added. Since the Cu partitioning coefficients only varied by 3.25 fold among treatments

406 on day 21 (LC-DFB: 0.065 vs. HC+DFB: 0.047; data not shown), we hypothesize that high CO_2 did not affect the

407 partitioning between particulate and dissolved Cu, but instead, it affected the speciation of dissolved Cu, increasing free

408 Cu (Cu^{2+}) and thus, its bioavailability. This resulted in the highest Cu:P ratios in the high CO_2 treatments, despite the

409 low phytoplankton biomass. This increase in bioavailability under lower pH is typical of metals that form strong

410 inorganic complexes with carbonates, such as Cu^{2+} (Millero et al., 2009). Thus in our future oceans, high CO_2 (low pH)

411 will shift the speciation of dissolved Cu towards higher abundance of free ionic species, increasing its bioavailability

412 and likely its toxicity.

413

414 Similarly to Cu, particulate Co, Zn and Mn were correlated with biomass and were dominated by the biogenic

415 component. But in contrast to Cu, these metals particulate concentrations were affect by increased CO_2 and/or the DFB

416 addition. However, the effects of high CO_2 and/or DFB were very complex because significant interactions between

417 these 2 factors were observed (Table 1); and further studies are required before we are able to discern and conclude a

418 significant trend. Yet, the P-normalized ratios of Co, Zn and Mn were significantly affected by CO_2 (Table 3),

419 exhibiting moderately lower ratios under high CO_2, when phytoplankton biomass was lowest. These results imply that

420 the bioavailability of these metals was not enhanced under acidic conditions. This suggests that under high CO_2 (low

421 pH) the free ionic species of these metals will not significantly increase in the future, as shown for metals that occur

422 predominantly as free ionic species in seawater (Millero et al., 2009).

423

5. Concluding remarks

The results presented here show that in the fjord where we carried out the present experiment, particulate Fe was dominated by lithogenic material, and was significantly decreased in the treatments with high CO_2 concentrations and/or the DFB addition. Indeed, high CO_2 and/or DFB promoted the dissolution of particulate Fe, and the presence of this strong organic complex helped maintaining high dissolved Fe. This shift between particulate and dissolved Fe, in the presence of DFB, promoted a massive bloom of *E. huxleyi* in the treatments with ambient CO_2, due to increased dissolved Fe. During the bloom of *E. huxleyi*, the concentrations of particulate metals (mol L^{-1}) with a strong biogenic component (Cu, Co, Zn, Cd, Mn, and Mo) were a) highly dynamic, b) positively correlated with plankton biomass, and c) influenced by growth requirements. Furthermore, high CO_2 decreased the Me:P ratios of Co, Zn and Mn, while increased the Cu:P ratios. In contrast DFB had no effects on these ratios. According to our results, high CO_2 may decrease particulate Fe and increase dissolved Fe, but high concentrations of dissolved Fe will only be maintained by the presence of strong organic ligands. The decrease in particulate Fe may affect the sinking flux of other metals associated with Fe oxides in open ocean settings. Furthermore, ocean acidification will decrease *E. huxleyi* abundance, and as a result, the sinking of particulate metals enriched in *E. huxleyi*. Moreover, the Me:P ratios of metals that are predominately present in an ionic free form in seawater (e.g. Co, Zn and Mn) will likely decrease or stay constant. In contrast, high CO_2 is predicated to shift the speciation of dissolved metals associated with carbonates, such as Cu, increasing their bioavailability, and resulting in higher Me:P ratios. We suggest that high Cu might be a common condition in this fjord, and autochthonous plankton might be able to cope with high Cu levels by developing specific physiological mechanisms. Future high CO_2 levels are expected to change the relative concentrations of particulate and dissolved metals, due to the differential effects of high CO_2 on trace metal solubility, speciation, adsorption and toxicity, as well as on the growth of different phytoplankton taxa, and their elemental trace metal composition.

Acknowledgments

This work was funded by CTM/MAR 2010-17216 (PHYTOSTRESS) research grant from the Spanish Ministry for Science and Innovation (Spain) to MS, and by NSERC grants (Canada) to MTM and JTC. MRL was funded by a FPU grant from the Ministry for Education (Spain) and by fellowships associated to the mentioned above research grants to carry out a short-stay at MTM and JTC laboratories to analyze dissolved and particulate metals. We thank all the participants of the PHYTOSTRESS experiment for their collaboration, and the MBS (Espegrend, Norway) staff for logistic support during the experiment.

References

Ahner, B.A., Liping, W., Oleson, J.R., Ogura, N.: Glutathione and other low molecular weight tiols in marine phytoplankton under metal stress, Mar. Ecol. Prog. Ser., 232, 93-103, 2002.

Behrenfeld, M.J., Milligan, A.J.: Photophysiological expressions of iron stress in phytoplankton, Ann. Rev. Mar. Sci. 5, 217–246, 2013.

Canadell, J.G., Quéré, C., Raupach, M.R., Field, C.B., Buitenhuis, E.T., Ciais, P., Conway, T.J., Gillet, N.P., Houghton, R.A., Marland, G.: Contributions to accelerating atmospheric CO_2 growth from economic activity, carbon intensity, and efficiency of natural sinks. Proc. Natl. Acad. Sci. USA 104, 18886-18870, 2007

Crawford, D.W., Lipsen, M.S., Purdie, D.A., Lohan, M.C., Statham, P.J., Whitney, F.A., Putland, J.N., Johnson, W.K., Sutherland, N., Peterson, T.D., Harrison, P.J., Wong, C.S.: Influence of zinc and iron enrichments on phytoplankton growth in the northeastern subarctic Pacific. Limnol. Oceanogr, 48,1583–1600, 2003.

Cullen, J.T., Sherrell, R.M.: Effects of dissolved carbon dioxide, zinc, and manganese on the cadmium to phosphorus ratio in natural phytoplankton assemblages, Limnol. Oceanogr. 50, 1193–1204, 2005.

Desboeufs, K.V. A. Sofikitis, R. Losno, J.L. Colin, P. Ausset. 2005. Dissolution and solubility of trace metals from natural and anthropogenic aerosol particulate matter Chemosphere 58 (2): 195-203 DOI: 10.1016/j.chemosphere.2004.02.025

Dymond, J., Lyle, M.: Flux comparisons between sediments and sediment traps in the eastern tropical Pacific: implications for atmospheric CO_2 variations during the Pleistocene. Limnol. Oceanogr, 30, 699–712, 1985

473 Field, C.B.: Primary production of the biosphere: Integrating terrestrial and oceanic components, Science 281, 237–240,
474   1998.
475 Frew, R.D., Hutchins, D.A., Nodder, S., Sanudo-Wilhelmy, S., Tovar-Sanchez, A., Leblanc, K., Hare, C.E., Boyd,
476   P.W.: Particulate iron dynamics during Fe Cycle in subantarctic waters southeast of New Zealand, Glob. Biogeochem.
477   Cycles 20, GB1S93. http://dx. doi.org/10.1029/2005GB002558, 2006.
478 Guo, J., Lapi, S., Ruth, T.J., Maldonado, M.T.: The effects of iron and copper availability on the copper stoichiometry
479   of marine phytoplankton. J. Phycol, 48, 312–325, 2012.
480 Ho, T-Y.: The trace metal composition of marine microalgae in cultures and natural assemblages. In: Rao S (ed) Algal
481   cultures, analogues of blooms and applications, Science Publishers, New Hampshire, p 271–299, 2006.
482 Ho, T., Quigg, A., Zoe, V., Milligan, A.J., Falkowski, P.G., Morel, M,M.: The elemental composition of some marine
483   phytoplankton. J. Appl. Phycol 1159,1145–1159, 2003
484 Ho, T-Y., Wen, L-S., You, C-F., Lee, D-C.: The trace metal composition of size-fractionated plankton in the South
485   China Sea: Biotic versus abiotic sources. Limnol. Oceanogr, 52, 1776–1788, 2007.
486 Ho, T-Y., You, C.F., Chou, W-C., Pai, S-C., Wen, L-S., Sheu, D.D.: Cadmium and phosphorus cycling in the water
487   column of the South China Sea: The roles of biotic and abiotic particles, Mar. Chem. 115-125-133, 2009.
488 Hoffmann, L.J., Breitbarth, E., Boyd P.W., Hunter, K.A.: Influence of ocean warming and acidification on trace metal
489   biogeochemistry, Mar Ecol Prog Ser 470-191–205, 2012.
490 Hutchins, D., Mulholland, M., Fu, F.: Nutrient cycles and marine microbes in a CO_2-enriched ocean, Oceanography
491   22-128–145, 2009.
492 Hutchins DA (2011) Forecasting the rain ratio. Nature 476: 41−42
493 Jakuba, R.W., Moffett, J.W., Dyhrman, S.T.: Evidence for the linked biogeochemical cycling of zinc, cobalt, and
494   phosphorus in the western North Atlantic Ocean, Global Biogeochem. Cycles 22, GB4012, 2008.
495 King, A.L., Sanudo-Wilhelmy, S.A., Boyd, P.W., Twining, B.S., Wilhelm, S.W., Breene, C., Ellwood, M.J. and
496   Hutchins, D.A.: A comparison of biogenic iron quotas during a diatom spring bloom using multiple approaches,
497   Biogeosciences 9, 667–687, 2012.

498 Kuma K, Nishioka J, Matsunaga K. Controls on iron(III) hydroxide solubility in seawater: the influence of pH and
499   natural organic chelators. Limnol Oceanogr 41:396−407.1996.

500 Lorenzo MRL, Iñiguez C, Egge J, Larsen A, Berger SAB, Garcia-Gomez C, Segovia M. Increased CO2 and iron
501   availability effects on carbon assimilation and calcification on the formation of Emiliania huxleyi blooms in a coastal
502   phytoplankton community.Env. Exp. Bot. 148:47-58, 2018.

503 Mackey, K.R.M., Morris, J.J., Morel, F.M.M.: Response of photosynthesis to ocean acidification, Oceanography 28,74–
504   91, 2015.
505 Marchetti A, Maldonado MT. Iron. In: Borowitzka MA, Beardall J, Raven JA (eds) The physiology of microalgae.
506   Springer International Publishing, Cham,, p 233–279.2016.
507
508 Millero, FJ, Sotolongo, S & Izaguirre, M. The oxidation kinetics of Fe(II) in seawater .Geochim. Cosmochim. Acta,51,
509   793-801. 1987.
510
511 Millero, F.J., Woosley, R., Ditrolio, B., Waters, J.: Effect of ocean acidification on the speciation of metals in seawater,
512   Oceanography 22:72–85, 2009.
513 Morel, F.M., Price, N.M.: The biogeochemical cycles of trace metals in the oceans, Science 300, 944–947, 2003.
514 Muller, F.L., Larsen, A., Stedmon, C.A., Søndergaard, M.: Interactions between algal – bacterial populations and trace
515   metals in fjord surface waters during a nutrient-stimulated summer bloom, Limnol Oceanogr 50, 1855–1871, 2005.

516 Öztürk M, Steinnes E, Sakshaug E. Iron speciation in the Trondheim Fjord from the perspective of iron limita- tion for
517   phytoplankton. Estuar Coast Shelf Sci 55:197−212. 2002.

518 Paasche, E.: A review of the coccolithophorid *Emiliania huxleyi* (Pymnesiophyceae), with particular reference to
519   growth, coccolith formation, and calcification-photosynthesis interactions, Phycologia 40, 503–529, 2002.
520 Price, N.M., Morel, F.M.M.: Cadmium and cobalt substitution for zinc in a marine diatom, Nature 344, 658–660, 1990.
521 Rauschenberg, S., Twining, B.S.: Evaluation of approaches to estimate biogenic particulate trace metals in the ocean,
522   Mar Chem 171, 67-77, 2015
523 Riebesell, U., Tortell, P.D.: Effects of ocean acidification on pelagic organisms and ecosystems, In: Gatusso J-P,
524   Lansson L (eds) Ocean Acidification. Oxford University Press., Oxford, p 99–121, 2011.
525 Robbins, L.L., Hansen, M.E., Kleypas, J.A., Meylan, S.C.: CO_2calc: A User Friendly Carbon Calculator foe Windows,
526   Mac OS X and iOS (iPhone), Open File Rep. 2010-1280, 2010.
527 Sanudo-Wilhelmy, S.A., Tovar-Sanchez, A., Fu, F.X., Capone, D.G., Carpenter, E.J., Hutchins, D.A.: The impact of
528   surface-adsorbed phosphorus on phytoplankton Redfield stoichiometry, Nature 432, 897–901, 2004.
529 Semeniuk, D.M, Bundy, R.M., Posacka, A.M., Robert, M., Barbeau K.A., Maldonado, M.T.: Using [67]Cu to study the
530   biogeochemical cycling of copper in the northeast subarctic Pacific ocean, Frontiers Mar. Sci. 3, 2-19, 2016.

531   Segovia, M., Lorenzo, M.R., Maldonado, M.T., Larsen, A., Berger, S.A., Tsagaraki, T.M., Lázaro, F.J., Iñiguez, C.,
532   García- Gómez, C., Palma, A., Mausz, M.A., Gordillo, F.J.L., Fernández, J.A., Ray, J. L., Egge, J.K.: iron availability
533   modulates the effects of future CO_2 levels within the marine planktonic food web, Mar. Ecol. Progr. Ser. 565, 17–33,
534   2017.
535   Segovia M, M Rosario Lorenzo, Concepción Iñiguez, Candela García-Gómez. Physiological stress response associated
536   with elevated CO_2 and dissolved iron in a phytoplankton community dominated by the coccolithophore Emiliania
537   huxleyi Marine. Ecol.Progr. Ser. 586: 73–89.2018.
538   Shi, D., Xu, Y., Hopkinson, B.M., Morel, F.M.M.: Effect of ocean acidification on ironavailability to marine
539   phytoplankton, Science 327, 676–679, 2010.
540   Stocker, T.F., Qin, D., Plattner, G-K., Tignor, M., Allen, S.K., Boschung, J., Nauels, A., Xia, Y., Bex, V., Midgley,
541   P.M. (Eds) IPCC, 2013: Climate Change 2013: The Physical Science Basis. Contribution of Working Group I to the
542   Fifth Assessment Report of the Intergovern- mental Panel on Climate Change. Cambridge University Press,
543   Cambridge, United Kingdom and New York, NY, USA, 2013.
544   Sunda, W.G., Huntsman, S.A.: iron uptake and growth limitation in oceanic and coastal phytoplankton, Mar. Chem. 50,
545   189–206, 1995a.
546   Sunda, W.G., Huntsman, S.A.: Cobalt and zinc interreplacement in marine phytoplankton: biological and geochemical
547   implications, Limnol. Oceanogr. 40, 1404–1417, 1995b.
548   Sunda, W.G., Huntsman, S.A. Control of Cd concentrations in a coastal diatom by interactions among free ionic Cd,
549   Zn, and Mn in seawater, Environ Sci Technol 32:2961–2968, 1998.
550   Sunda, W.G., Huntsman, S.A.: Effect of Zn, Mn, and Fe on Cd accumulation in phytoplankton: implications for oceanic
551   Cd cycling, Limnol. Oceanogr. 45, 1501–1516, 2000.
552   Sunda, W.G.: Feedback interactions between trace metal nutrients and phytoplankton in the ocean, Front Microbiol 3,
553   204, 2012.
554   Tang, D.G.,Morel, F.M.M.: Distinguishing between cellular and Fe-oxide-associated trace elements in phytoplankton,
555   Mar. Chem. 98, 18–30, 2006.
556   Taylor, S.: Abundance of chemical elements in the continental crust: a new table. Geochim Cosmochim Acta 28, 1273–
557   1285, 1964.
558   Tovar-Sanchez, A., Sanudo-Wilhelmy, S.A., Garcia-Vargas, M., Weaver, R.S., Popels, L.C., Hutchins, D.A.: A trace
559   metal clean reagent to remove surface-bound iron from marine phytoplankton, Mar. Chem. 82, 91–99, 2003.
560   Tovar-Sanchez, A., Sanudo-Wilhelmy, S.A., Kustka, A.B., Agustí, S., Dachs, J., Hutchins, D.A., Capone, D.G. and
561   Duarte, C.M.: Effects of dust deposition and river discharges on trace metal composition of Trichodesmium spp. in
562   the tropical and subtropical North Atlantic Ocean, Limnol Oceanogr 51, 1755–61, 2006.
563   Twining, B.S., Baines, S.B.: The trace metal composition of marine phytoplankton, Ann Rev Mar Sci 5, 191–215,
564   2013.
565   Xu, Y., Tang, D., Shaked, Y., Morel, F.M.M.: Zinc, cadmium, and cobalt interreplacement and relative use efficiencies
566   in the coccolithophore *Emiliania huxleyi*, Limnol Oceanogr 52, 2294–2305, 2007.
567   Zamzow, H., Coale, K.H., Johnson, K.S.,Sakamoto, C.M.: Determination of copper complexation in seawater using
568   flow injection analysis with chemiluminescence detection, Anal Chim Acta 377, 133–144, 1998.
569   Zondervan, I.: The effects of light, macronutrients, trace metals and CO_2 on the production of calcium carbonate and
570   organic carbon in coccolithophores–A review, Deep Sea Res Part II Top Stud Oceanogr 54,521–537, 2007.

Table 1. Statistical analyses (Split-plot ANOVA) of the effects of high CO_2, the addition of DFB, and their interaction, as well as the effect of time, on the concentrations of particulate metals (mmol L^{-1}, data in Table S2, and Figure 3) in particles collected from the different mesocosms treatments.

Factor	Al	Ti	P	Fe	Cu	Co	Zn	Cd	Mn	Mo	Pb
CO_2	ns	ns	**	*	ns	**	***	***	**	***	ns
DFB	ns	ns	*	ns	ns	*	**	ns	*	*	ns
CO_2 x DFB	ns	*	**	ns	ns	*	**	*	**	**	ns
Time	ns	ns	ns	***	*	***	***	***	***	***	**

*ns: not significant; * p <0.05; ** p <0.01; *** p<0*

Table 2. The average metal ratios in the particles collected in this study (without oxalate wash) using the data reported in Table S2. The P-normalized ratios (mmol : mol P, Figure 4) are compared to previous estimates in marine plankton samples and phytoplankton cultures (A). The Al-normalized ratios (mmol : mol Al) are compared to crustal ratios (B).

A)

(mmol : mol P)	Mn:P	Fe:P	Co:P	Cu:P	Zn:P	Cd:P	Mo:P	Al:P	Reference
Phytoplankton Lab	3.8	7.5	0.19	0.38	0.8	0.21	0.03		Ho et al. 2003
Marine Plankton Field	0.68±0.54	5.1±1.6	0.15±0.06	0.41±0.16	2.1±0.88				Ho 2006
E. huxleyi Lab	7.1±0.36	3.5±0.07	0.29±0.02	0.07±0.013	0.38±0.002	0.36±0.01	0.022±0.0003		Ho et al. 2003
This study	1.65±0.41	39.2±34.3	0.07±0.02	1.41±0.55	34.02±18.05	0.02±0.01	0.42±0.12	70±38	
Crust ratio	510	29,738	13	25	32	0.05	0.46	89,972	Taylor 1964

B)

(mmol : mol Al)	Mn:Al	Fe:Al	Co:Al	Cu:Al	Zn:Al	Cd:Al	Mo:Al	Pb:Al	Ti:Al
Crustal ratio	5.7	331	0.14	0.27	0.35	0.001	0.005	0.02	39
This study	35±28	506±342	1.5±1.2	26.5±15	795±865	0.5±0.4	8.6±6.5	4.9±3.9	119±47.6

Table 3. Statistical analyses (Split-plot ANOVA) of the effects of CO_2, DFB, and their interaction, as well as the effect of time, on the P-normalized metal quotas (mmol: mol P, data in Figure 4, and Table S2) in particles collected from the different mesocosm treatments.

Factor	Fe:P	Cu:P	Co:P	Zn:P	Cd:P	Mn:P	Mo:P	Pb:P	Ti:P
CO_2	ns	*	***	**	ns	*	ns	ns	ns
DFB	ns	ns	ns	ns	ns	ns	ns	ns	ns
CO_2 x DFB	ns	ns	ns	ns	ns	ns	ns	ns	ns
Time	***	***	***	***	ns	ns	ns	ns	***

*ns: not significant; * p <0.05; ** p <0.01; *** p<0.001*

Table 4. The relationship (Pearson correlations, $p < 0.05$) between particulate metals concentrations (nmol L^{-1}, no oxalate wash, reported in Table S2) and the biomass ($\mu gC\ L^{-1}$) of *Emiliania huxleyi* and total cells (phytoplankton and microzooplankton) collected from the different mesocosm treatments.

		P	Fe	Cu	Co	Zn	Cd	Mn	Mo	Pb	Ti
E. huxleyi	Correlation coefficient	0.622	ns	0.614	0.756	0.747	0.818	0.686	0.825	ns	ns
	P-value	0.003		0.003	$7.35 \cdot 10^{-5}$	$1.01 \cdot 10^{-4}$	$6.02 \cdot 10^{-6}$	$5.93 \cdot 10^{-4}$	$4.20 \cdot 10^{-6}$		
Total cells	Correlation coefficient	0.641	ns	0.51	0.644	0.889	0.802	0.598	0.53	ns	ns
	P-value	0.002		0.02	$1.62 \cdot 10^{-3}$	$7.03 \cdot 10^{-8}$	$1.23 \cdot 10^{-5}$	$4.18 \cdot 10^{-3}$	$1.35 \cdot 10^{-2}$		
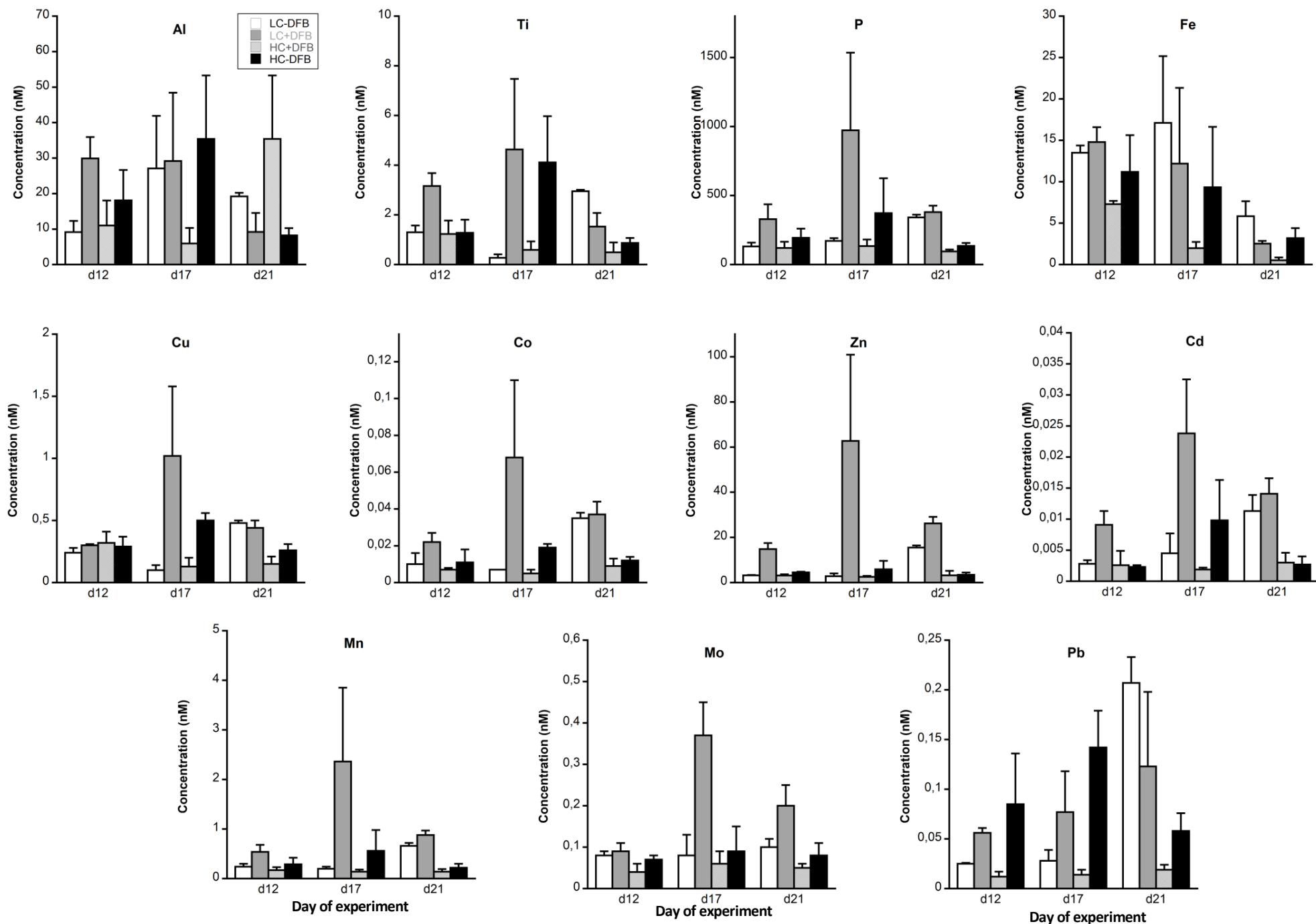
Fig. 1. The concentration of particulate metals in seawater (nM) in the different treatments; LC: ambient CO_2 (390 µatm); HC: increased CO_2 (900 µatm); -DFB (ambient dFe); +DFB (increased dFe) during the development of a bloom of Emiliania huxleyi. Bars are means of measurements in 3 independent mesocosms (n = 3) except for LC−DFB where n = 2. Error bars indicate SD.
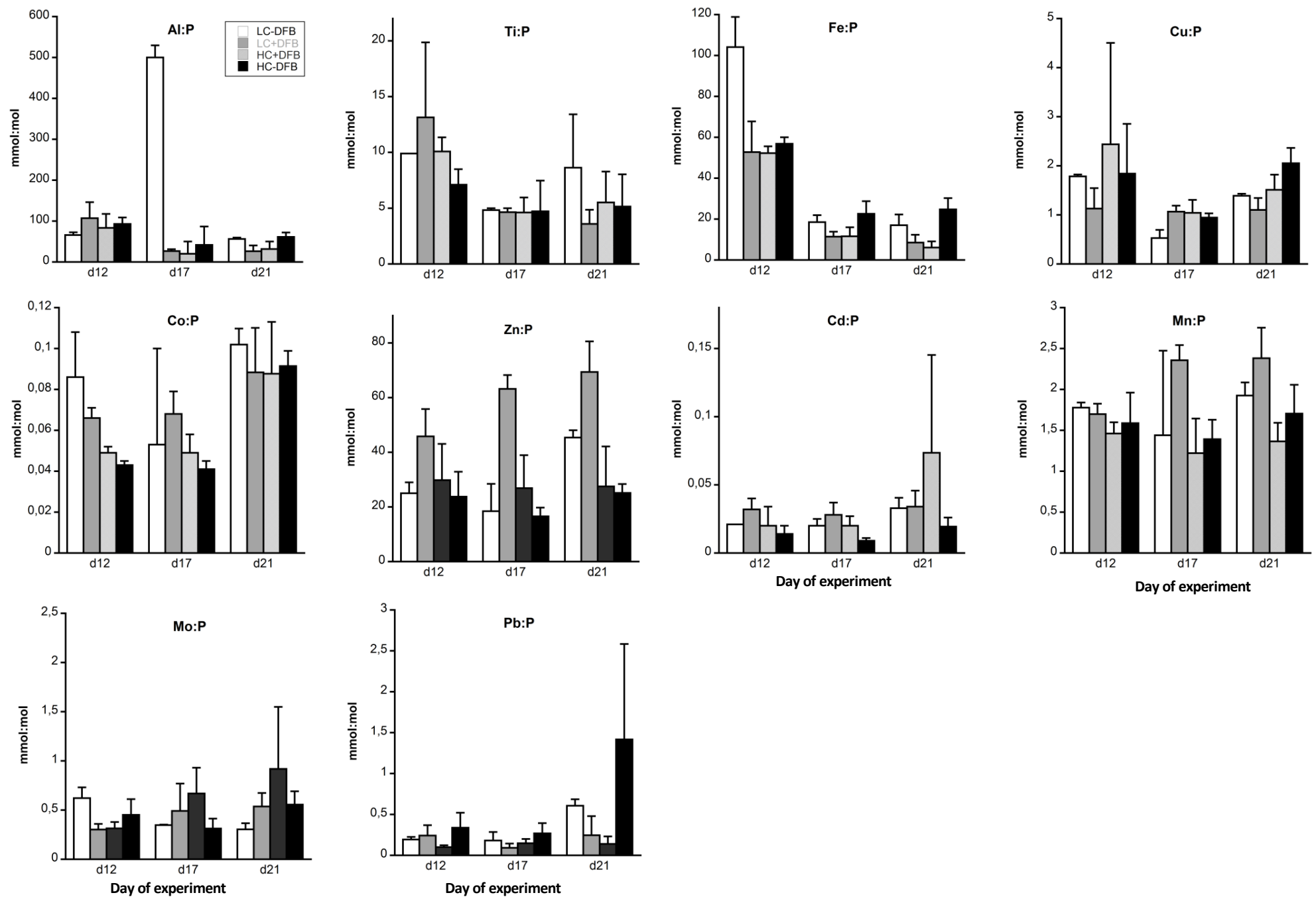
Fig. 2. P-normalized metal quotas (mmol:mol P) of particles from different treatments; LC: ambient CO_2 (390 µatm); HC: increased CO_2 (900 µatm); -DFB (ambient dFe); +DFB (increased dFe) during the development of a bloom of *Emiliania huxleyi*. Bars are means of measurements in 3 independent mesocosms (n = 3) except for LC−DFB where n = 2. Error bars indicate SD.
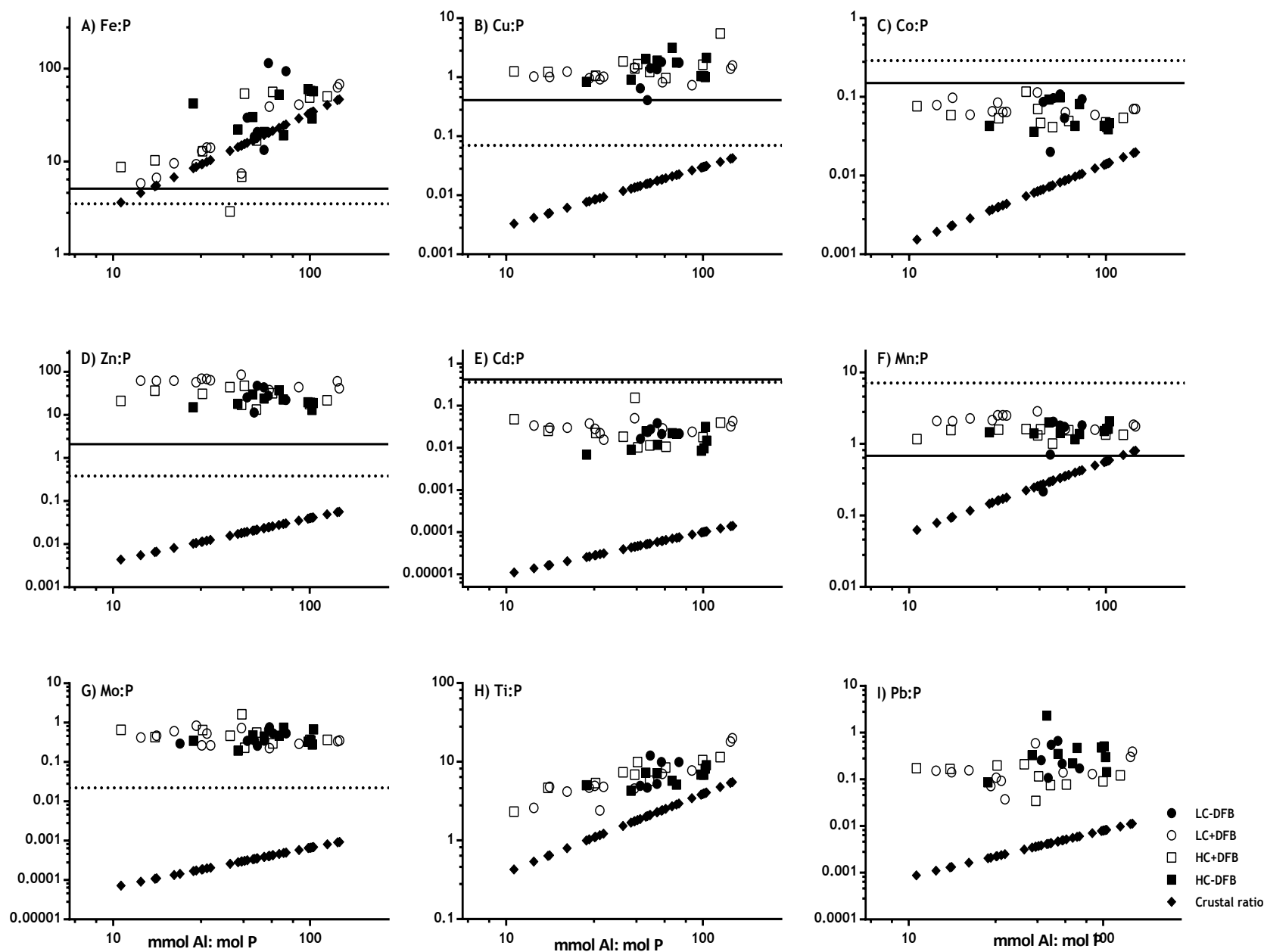
Fig. 3. Comparison of P-normalized metal ratios in particles (mmol:mol P) against mmol Al:mol P ratios in the same particles (without oxalate wash) collected from the different mesocosm treatments (LC: ambient CO_2; HC: increased CO_2 (900 μatm); -DFB: no DFB addition; +DFB: with a 70 nM DFB addition) during the development of a bloom on day 12, 17 and 21 (original data reported in Table S2). The x-axis parallel solid and dotted lines represent the average metal quotas obtained from marine plankton assemblages (Ho 2006) and from cultures of *Emiliania huxleyi* (Ho et al. 2003). The slope of the line with the ♦ symbols indicates the average metal : Al (mol:mol) in crustal material (Taylor, 1964). (A) Fe:P, (B) Cu:P, (C) Co:P, (D) Zn:P, (E) Cd:P, (F) Mn:P, (G) Mo:P, (H) Ti:P, (I) Pb:P.
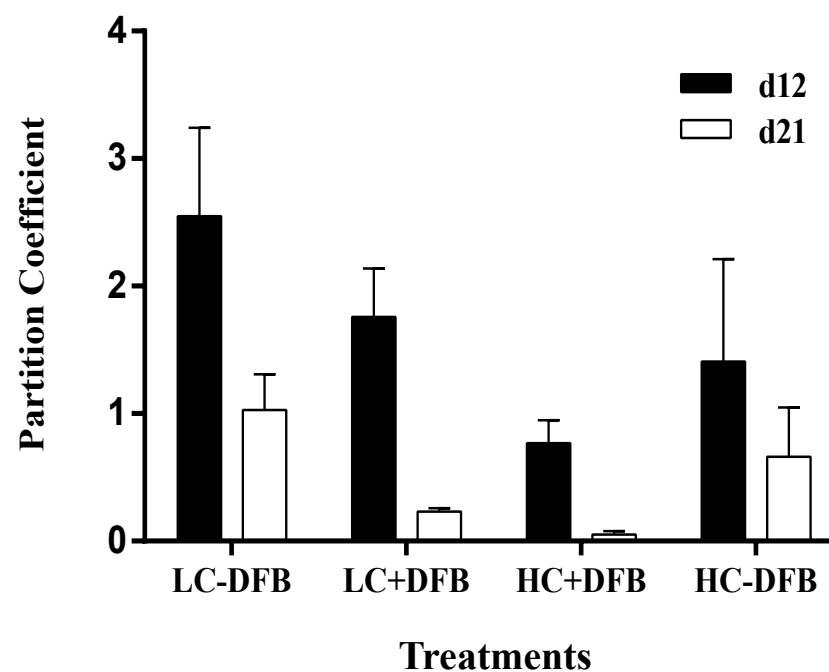
Fig. 4. The Fe partition coefficients (the molar ratio between particulate and dissolved concentrations) in the different mesocosm treatments; LC: ambient CO_2 (390 µatm); HC: increased CO_2 (900 µatm); -DFB: no DFB addition; +DFB: with a 70 nM DFB addition; on day 12 and day 21. . Bars are means of measurements in 3 independent mesocosms (n = 3) except for LC−DFB where n = 2. Error bars indicate SD.